Analyst

ROYAL SOCIETY OF CHEMISTRY

PAPER

View Article Online
View Journal | View Issue

Cite this: *Analyst*, 2021, **146**, 1872

In vitro measurement of superoxide dismutase-like nanozyme activity: a comparative study†

Yufeng Liu, [a] Yihong Zhang,[a] Quanyi Liu,[b] Quan Wang,[a] Anqi Lin, [a] Jie Luo,[c] Yan Du, [b] Ying-Wu Lin [c] and Hui Wei *[a,d,e]

Analyzing the SOD-like activity of nanozymes *in vitro* is of great importance for identifying new nanozymes and predicting their potential biological effects *in vivo*. However, false negative or positive results occasionally occur due to the mismatch between the detection methods and nanozymes. Here, five typical SOD-like nanozymes, including CeO_2, Mn_3O_4, Prussian blue (PB), PCN222-Mn, and Pt NPs, have been used to evaluate the sensitivity and accuracy of several commonly used *in vitro* detection methods. By systematically analyzing the detection results, several precautions have been taken. (1) The hydroethidine (HE) probe could be disturbed by the nanozyme with oxidative ability. (2) The nitro blue tetrazolium (NBT) probe has a moderate sensitivity due to the poor water solubility of its reduced product. (3) The water-soluble tetrazolium salt (WST)-8 probe has a higher sensitivity than both NBT and iodonitrotetrazolium chloride (INT). (4) The detection system using the irradiation of riboflavin to produce $^{\bullet}O_2^-$ might be interfered by the nanozyme with photosensibility. (5) Both the quality of DMPO and incubation time are important factors for electron paramagnetic resonance (EPR) measurement. This study will be useful for choosing more suitable *in vitro* detection methods of SOD-like activity for nanozymes in the future.

Received 1st November 2020,
Accepted 31st December 2020

DOI: 10.1039/d0an02164d

rsc.li/analyst

Introduction

Reactive oxygen species (ROS), including superoxide anions ($^{\bullet}O_2^-$), hydroxyl radicals ($^{\bullet}OH$), singlet oxygen ($^1O_2$), and hydrogen peroxide (H_2O_2), are generated during the metabolism of oxygen and play very important roles in diseases such as cardiovascular disease,[1] inflammatory bowel disease,[2] rheumatoid arthritis,[3] and even cancer.[4] To protect tissues from dysregulated ROS-induced damage (*e.g.*, oxidative stress), living organisms have the corresponding evolved enzymes to regulate the abnormal levels of ROS.[5] Among them, superoxide dismutase (SOD) is an important antioxidant enzyme for catalyzing the dismutation of $^{\bullet}O_2^-$ into molecular oxygen and H_2O_2. In addition, using SODs as therapeutic agents against ROS-related diseases has been successfully established.[6] For instance, SODs are found to be effective for the treatment of myocardial ischemia–reperfusion injury,[7] multiple myeloma,[8] and several kinds of inflammatory diseases.[9] Although SODs have efficient ROS scavenging ability, high cost and low stability have limited their applications. To date, lots of efforts have been contributed to developing SOD mimics to overcome the drawbacks of enzymatic counterparts.[10–12] Among them, nanomaterials with SOD-like activity (called SOD-like nanozymes) have received particular interest due to their low cost, high stability, and efficient therapeutic effect *in vivo*.[12–15]

For SOD-like nanozymes, analyzing their *in vitro* activities is not only beneficial for predicting potential therapeutic effects *in vivo*, but also provides an effective screening method for identifying on-demand nanozymes from the available nanomaterials. Due to the high activities of $^{\bullet}O_2^-$ for both oxidation and reduction, different types of probes have been used as indicators through the redox reactions with $^{\bullet}O_2^-$.[16,17] However, these redox reaction based detection methods have limited specificity for evaluating the $^{\bullet}O_2^-$ scavenging abilities of nanozymes due to the possible competitive reactions between nanozymes/probes and $^{\bullet}O_2^-$/probes. Such a mismatch between a probe and a SOD-like nanozyme would generate a false positive or negative result, seriously interfering with the measure-

[a]*Department of Biomedical Engineering, College of Engineering and Applied Sciences, Nanjing University, Nanjing, Jiangsu 210023, China. E-mail: weihui@nju.edu.cn*
[b]*State Key Laboratory of Electroanalytical Chemistry, Changchun Institute of Applied Chemistry, Chinese Academy of Science, Changchun, Jilin 130022, China*
[c]*Laboratory of Protein Structure and Function, School of Chemistry and Chemical Engineering, University of South China, Hengyang, Hunan 421001, China*
[d]*Nanjing National Laboratory of Microstructures, Jiangsu Key Laboratory of Artificial Functional Materials, Nanjing University, Nanjing, Jiangsu 210093, China*
[e]*State Key Laboratory of Analytical Chemistry for Life Science, School of Chemistry and Chemical Engineering, Chemistry and Biomedicine Innovation Center (ChemBIC), Nanjing University, Nanjing, Jiangsu 210023, China*

†Electronic supplementary information (ESI) available. See DOI: 10.1039/d0an02164d

ments. In this regard, it is urgent to ensure that the measurement of SOD-like activity is suitable for the corresponding nanozyme.

To tackle this challenge, herein, several probes have been selected to detect the *in vitro* SOD-like activities of five typical SOD-like nanozymes (CeO_2,[18] Mn_3O_4,[19] Prussian blue (PB),[20] PCN222-Mn,[21] and Pt NPs[22]). Two methods (one is the xanthine (X)/xanthine oxidase (XO) method and the other is the irradiation of riboflavin method) are used to produce $^{\bullet}O_2^-$. The selected probes are hydroethidine (HE),[23] nitro blue tetrazolium (NBT),[24] iodonitrotetrazolium chloride (INT),[25] water-soluble tetrazolium salts (WST)-8,[26] cytochrome *c*,[27] and 5,5-dimethyl-1-pyrroline-*N*-oxide (DMPO).[28] Through such a systematically comparative study, several useful precautions have been taken, which will be useful for choosing more suitable *in vitro* detection methods of SOD-like activity for nanozymes in the future.

Experimental section

Reagents and materials

Commercially available reagents were of analytical grade and were used without further purification. Manganese acetate ($Mn(OAc)_2$) was purchased from Shanghai Meixing Chemical Reagent Co., Ltd. Chloroplatinic acid ($H_2PtCl_6{\cdot}6H_2O$), NBT, X, XO, and diethylene triamine pentaacetic acid (DTPA) were obtained from Sigma-Aldrich. DMPO was obtained from Dojindo Co., Ltd. SOD assay kits (WST-8) and natural SODs were purchased from Beyotime Chemical Reagent Co., Ltd. Hydroethidine (HE), cerium nitrate hexahydrate, ethylene glycol, riboflavin, and ammonia solution were obtained from Aladdin Chemical Reagent Co., Ltd. $ZrOCl_2{\cdot}8H_2O$ was purchased from Energy Chemical Co. Ltd. INT was purchased from J&K Scientific Ltd. Cytochrome *c* was obtained from Shanghai Yuanye Biotechnology Co., Ltd. All aqueous solutions were prepared with deionized water (18.2 MΩ cm, Millipore).

Instrumentation

TEM imaging was performed on a Tecnai F20 microscope FEI (Field Electron and Iron Company) at an acceleration voltage of 200 kV. PXRD patterns were obtained with an ARL SCINTAC X′TRA diffractometer using Cu Kα radiation (Thermo Fisher Scientific). The spectra from both absorbance and fluorescence analyses were recorded on a microplate reader (SpectraMax M2e, Molecular Device Co. Ltd, Shanghai, China). A LED lamp (27 W) was used for the irradiation of riboflavin.

Synthesis of nanozymes (CeO_2, Mn_3O_4, PB, PCN222-Mn, and Pt NPs)

The nanozymes of CeO_2 and Mn_3O_4 were synthesized according to our previous work.[29] CeO_2 used was not freshly prepared.

The nanozyme of PB was synthesized as follows.[30] $K_4[Fe(CN)_6]$ (0.01 mmol) and citric acid (5 mmol) were dissolved in 20 mL of H_2O under stirring at 60 °C (solution A). Fe $(NO_3)_3{\cdot}9H_2O$ (0.05 mmol) and citric acid (5 mmol) were dissolved in 20 mL of H_2O (solution B). Solution B was added to solution A over 10 min, and the mixture was kept to react at 60 °C for another 5 min. The mixed solution was then cooled to room temperature and further stirred for 30 min. The mixture was centrifuged at 9000 rpm for 10 min and then washed three times with ethanol.

The nanozymes of PCN222-Mn and Pt NPs were synthesized according to our previous work.[21]

Measurements of SOD-like activities for nanozymes

Method of the HE probe

Production of $^{\bullet}O_2^-$ by using a mixture of X and XO. Typically, X (1.5 mM), XO (0.05 U mL^{-1}), and different concentrations of nanozymes were mixed in Tris-HCl buffer (0.1 M, pH 7.6) at 37 °C. The mixture was incubated for 10 min. Then, HE (0.1 mg mL^{-1}) was added to the solution for another 10 min reaction. Fluorescence spectra were recorded at an excitation wavelength of 470 nm.

Production of $^{\bullet}O_2^-$ by irradiating riboflavin. Typically, riboflavin (1.2 mM), EDTA (0.1 M), different concentrations of nanozymes, and HE (0.1 mg mL^{-1}) were mixed in Tris-HCl buffer (0.1 M, pH 7.6), and then irradiated under a LED lamp for 5 min. Fluorescence spectra were recorded at an excitation wavelength of 470 nm.

Method of the NBT probe

Production of $^{\bullet}O_2^-$ by using a mixture of X and XO. Typically, different concentrations of nanozymes were mixed with X (1.2 mM) and XO (0.05 U mL^{-1}) in Tris-HCl buffer (0.1 M, pH 7.6) at 37 °C for 5 min. Then, NBT (0.1 mg mL^{-1}) was added to the mixed solution for another 5 min, and the absorption spectra of the mixed solution were then obtained using a microplate reader.

Production of $^{\bullet}O_2^-$ by irradiating riboflavin. Typically, riboflavin (1.2 mM), EDTA (0.1 M), different concentrations of nanozymes, and NBT (0.1 mg mL^{-1}) were mixed in Tris-HCl buffer (0.1 M, pH 7.6), and then irradiated with a LED lamp for 5 min. The absorption spectra of the mixed solution were then obtained using a microplate reader.

Method of the INT probe. Typically, different concentrations of nanozymes were mixed with X (3 mM) and XO (0.05 U mL^{-1}) in Tris-HCl buffer (0.1 M, pH 7.6) at 37 °C for 5 min. Then, INT (0.05 mg mL^{-1}) was added to the mixed solution for another 5 min, and the absorption spectra of the mixed solution were then obtained using a microplate reader.

Method of the WST-8 probe (SOD assay kits). According to the protocol of SOD assay kits, the nanozyme (20 μL) was mixed with 160 μL of the WST-8/enzyme solution in a microplate well. Then, 20 μL of the starting solution was added. After incubation at 37 °C for 30 min, the absorbance at 450 nm was measured using a microplate reader.

Method of the cytochrome *c* probe. Typically, different concentrations of nanozymes were mixed with X (1.2 mM), XO (0.05 U mL^{-1}), cytochrome *c* (0.3 mg mL^{-1}), and catalase (1 mg mL^{-1}, 1 mg > 3000 U) in Tris-HCl buffer (0.1 M, pH 7.6)

at 37 °C for 10 min. Then, the absorption spectra were measured using a microplate reader.

Method of EPR

Method in Fig. 6. EPR spectra were recorded on a Bruker A300 spectrometer (X-band) at room temperature with a frequency of 9.256 GHz. The samples had the final concentrations of X (0.5 mM), XO (0.005 U), and DMPO (22.5 mg mL^{-1}) and different concentrations of nanozymes in PBS (0.1 M, pH 7.5) that contained DTPA (25 μM).

Method in Fig. S7†. EPR spectra were recorded on a Bruker EMX-10/12 spectrometer (X-band) at room temperature with a frequency of 9.772 GHz. The samples had a final concentration of X (0.5 mM), XO (0.05 U), and DMPO (22.5 mg mL^{-1}) in Tris-HCl buffer (0.1 M, pH 7.6) that contained DTPA (25 μM). The mixing times of the samples were 10 s, 30 s, 60 s, and 120 s, respectively.

Results and discussion

Synthesis and characterization of SOD-like nanozymes

Nanozymes with SOD-like activity have been developed as efficient therapeutic reagents for the treatment of ROS-related diseases. In this study, we synthesized five typical SOD-like nanozymes for evaluating the differences among several commonly used *in vitro* SOD activity detection methods. As shown in Fig. 1 and S1,† both TEM images and powder X-ray diffraction (PXRD) patterns of CeO_2, Mn_3O_4, PB, PCN222-Mn, and Pt NPs were consistent with previous reports.[21,29,30] The XRD patterns of CeO_2, Mn_3O_4, PB, and Pt NPs matched well with the standard patterns of ceria (JCPDS card no. 43-1002), Mn_3O_4 (JCPDS card no. 24-0734), PB (JCPDS card no. 73-0687), and Pt NPs (JCPDS card no. 87-0642), demonstrating the successful synthesis of these nanozymes. Moreover, to minimize the potential interference of nanozymes, the absorption spectra of nanozymes themselves with different concentrations have been obtained (Fig. S2†). As the HE-based fluorescence detection system needs to be excited at 470 nm, the corresponding fluorescence spectra of nanozymes themselves were obtained as well (Fig. S3†).

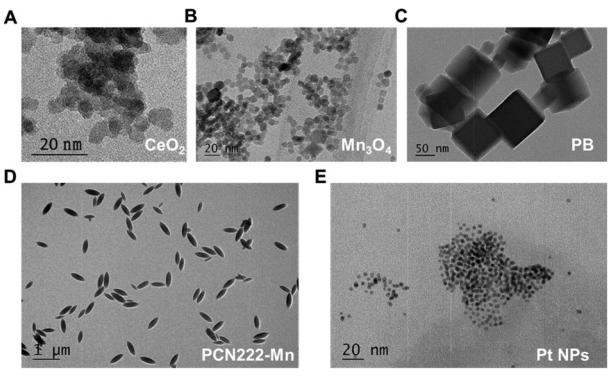

Fig. 1 TEM images of (A) CeO_2, (B) Mn_3O_4, (C) PB, (D) PCN222-Mn, and (E) Pt NPs.

In vitro detection methods of SOD-like activity

Generally, the detection of SOD-like activity can be divided into two steps. First, $^{\bullet}O_2^-$ is produced by using an appropriate method. Second, the amount of $^{\bullet}O_2^-$ eliminated by a nanozyme is measured. To generate $^{\bullet}O_2^-$, using a mixture of X and XO is a typically and widely used method due to the mild reaction conditions and the stable generating process. Besides, the irradiation of riboflavin as well as a solution containing potassium superoxide (KO_2) can also produce $^{\bullet}O_2^-$. Due to the insolubility of KO_2 in water, the enzyme method and the irradiation of riboflavin were chosen in our work for the production of $^{\bullet}O_2^-$ in aqueous solutions.

To measure the amount of $^{\bullet}O_2^-$, three kinds of probes including fluorescent, colorimetric, and electron spin resonance were used. As shown in Fig. 2, HE could be oxidized by $^{\bullet}O_2^-$ to produce fluorescence, while NBT, INT, WST-8, and cytochrome *c* could be reduced by $^{\bullet}O_2^-$ to generate their corresponding colored products. Unlike the $^{\bullet}O_2^-$ mediated redox reactions, DMPO is a spin trap to catch $^{\bullet}O_2^-$ and forms a more stable adduct for EPR measurement.

The five SOD-like nanozymes were tested using these probes and the two $^{\bullet}O_2^-$ generation methods for analyzing the precautions and application scope of each detection method.

HE

First, we evaluated the SOD-like activities of CeO_2, Mn_3O_4, PB, PCN222-Mn, and Pt NPs using HE and two $^{\bullet}O_2^-$ producing methods. As a sensitive $^{\bullet}O_2^-$ indicator, HE could be oxidized by $^{\bullet}O_2^-$ to produce a wide fluorescence spectrum range from

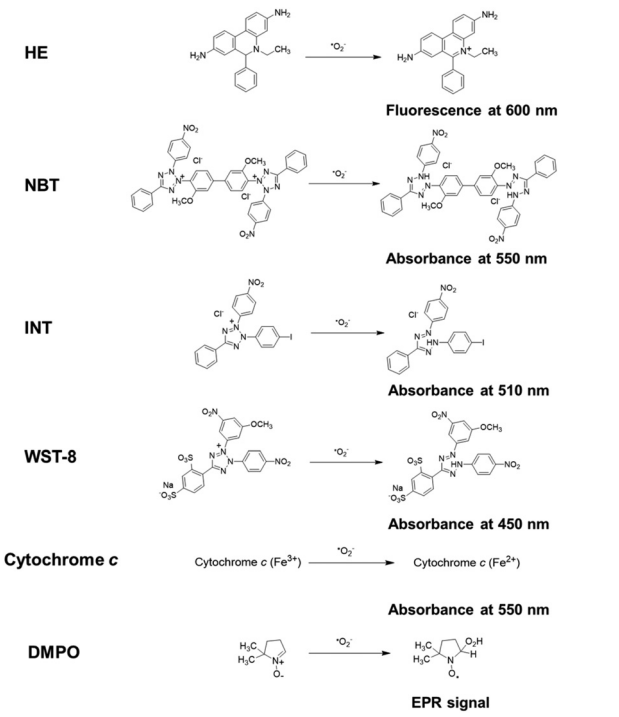

Fig. 2 Probes for the *in vitro* detection of SOD-like activity.

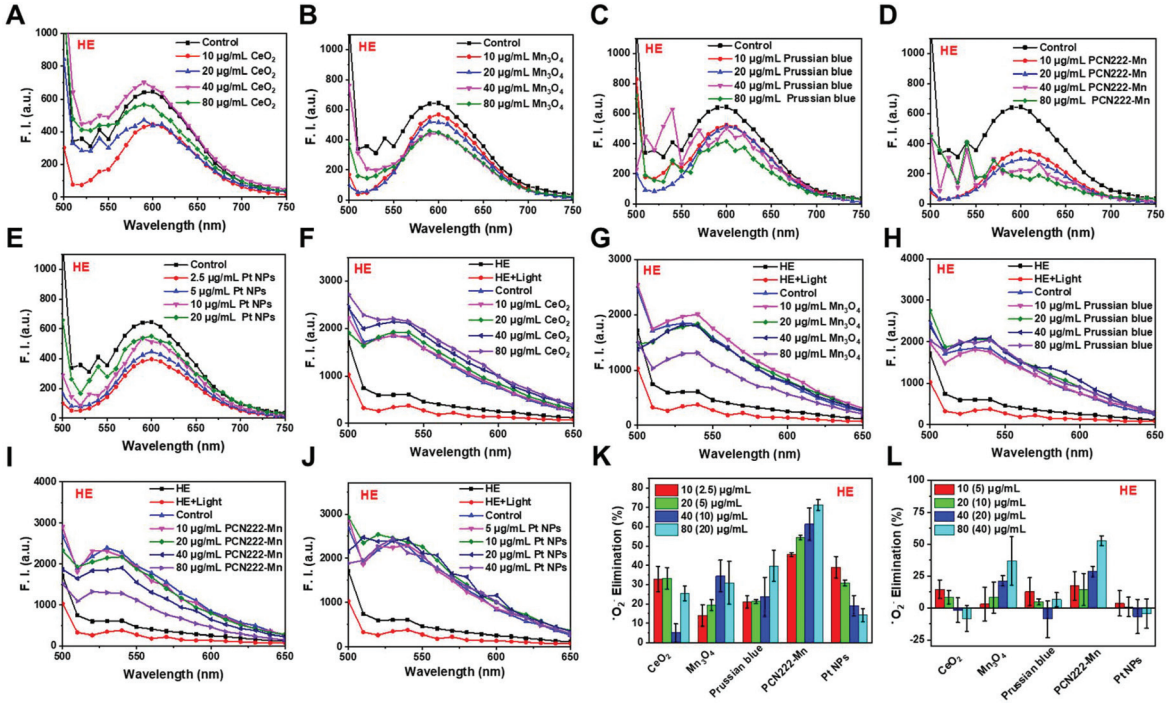

Fig. 3 Fluorescence spectra of the mixture of X, XO, and HE in the absence and presence of different concentrations of (A) CeO_2, (B) Mn_3O_4, (C) PB, (D) PCN222-Mn, and (E) Pt NPs. Fluorescence spectra of the mixture of HE and riboflavin under illumination for 5 min in the absence and presence of different concentrations of (F) CeO_2, (G) Mn_3O_4, (H) PB, (I) PCN222-Mn, and (J) Pt NPs. (K) Dependence between the elimination efficiency of $^{\bullet}O_2^-$ and the concentrations of nanozymes, data analyzed from panels A–E. (L) Dependence between the elimination efficiency of $^{\bullet}O_2^-$ and the concentrations of nanozymes, data analyzed from panels F–J. The data are shown as means ± SD (n = 3).

550 nm to 650 nm (typically centred at 600 nm). According to Fig. 3A–E and K, all nanozymes decreased the amount of $^{\bullet}O_2^-$ that was generated from the mixture of X and XO, showing their $^{\bullet}O_2^-$ scavenging abilities. Also, Fig. S5A and S5F† show that this detection system had an excellent sensitivity for natural SODs. However, unlike other nanozymes, PB and Pt NPs didn't show positive correlations between SOD-like activities and concentrations. High concentrations of PB and Pt NPs didn't enhance their activities, showing false negative results in this detection system. As we know, apart from $^{\bullet}O_2^-$, HE could be oxidized by other oxidants to produce non-specific fluorescence, which would disturb the tests of $^{\bullet}O_2^-$. At the same time, both PB and Pt NPs have been demonstrated with oxidase-like activities.[31,32] We reasoned that HE could be oxidized by high concentrations of PB and Pt NPs, and then the competitive reactions between nanozymes/HE and HE/$^{\bullet}O_2^-$ would affect the detection accuracy and generate inaccurate results. Therefore, it is necessary to take the oxidative ability of the nanozyme into consideration for the HE-based SOD detection system.

Apart from this, the irradiation of riboflavin, another $^{\bullet}O_2^-$ producing method, was also used to study the performance of the HE probe for detecting the SOD-like activities of these nanozymes. As shown in Fig. 3F–J and L, only Mn_3O_4 and PCN222-Mn showed SOD-like activities, indicating that the detection system has limited scope of application. Furthermore, the fluorescence of oxidized HE was seriously affected by the fluorescence of riboflavin. Moreover, the fluorescence of HE was decreased by irradiation, which means that HE is unstable under irradiation. Fig. S6A and S6C† show that this method is not suitable for the detection of natural SODs either. To this end, the enzyme method for $^{\bullet}O_2^-$ production is more suitable for the HE probe than the irradiation method.

NBT

NBT, a widely used probe for the detection of SOD-like activity, could be specifically reduced by $^{\bullet}O_2^-$ to produce a wide absorption spectrum from 450 nm to 700 nm (typically centred at 550 nm). Natural SODs and the nanozymes of CeO_2, Mn_3O_4, PB, PCN222-Mn, and Pt NPs were then investigated using NBT as an indicator. A mixture of X and XO was used to generate $^{\bullet}O_2^-$. As shown in Fig. 4A–E and K, by analysing the changes of absorbance at 550 nm, the SOD-like activities of Mn_3O_4, PCN222-Mn, and Pt NPs were demonstrated. However, CeO_2 and PB didn't show SOD-like activities, indicating false negative results and the limited detection sensitivity of this detection method. In this detection, because the reduced product of the NBT probe has poor water solubility, it is recommended that the absorbance at 550 nm in the control group does not exceed 0.8. Besides, this detection system also exhibited moderate sensitivity for natural SODs (Fig. S5B and S5F†). We reasoned that the limited changes of absorbance decreased the sensitivity of the NBT probe. Therefore, taking into consideration the balance between the water solubility of the

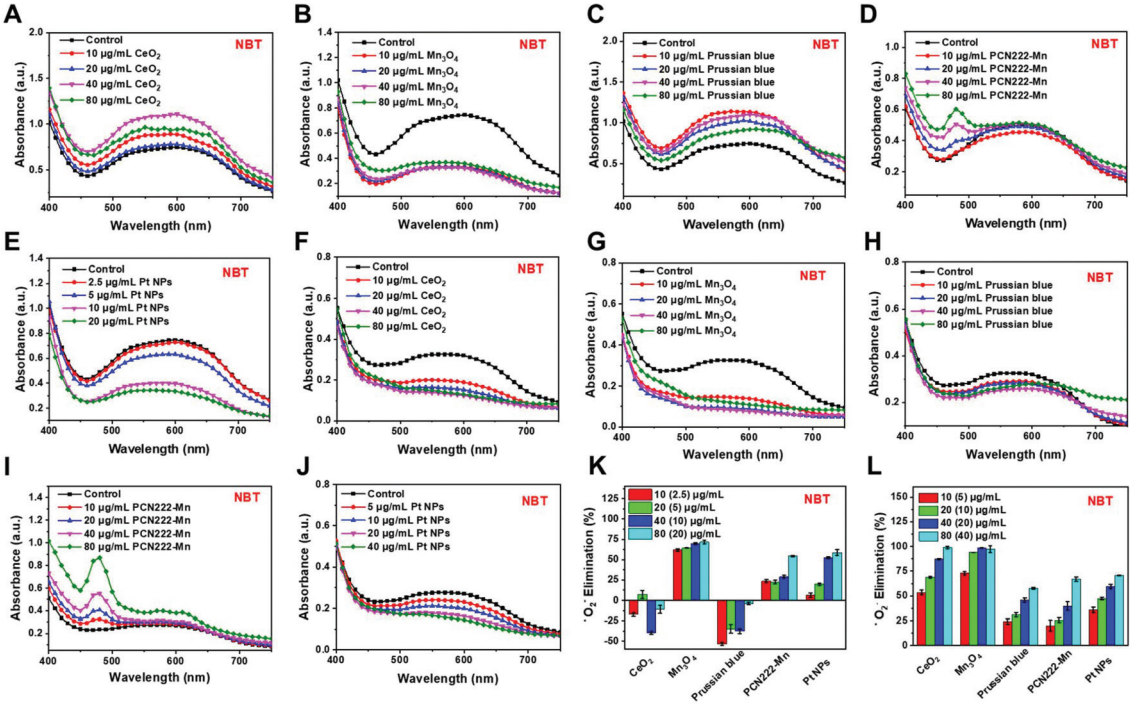

Fig. 4 Absorption spectra of the mixture of NBT with X and XO in the absence and presence of different concentrations of (A) CeO_2, (B) Mn_3O_4, (C) PB, (D) PCN222-Mn, and (E) Pt NPs. Absorption spectra of the mixture of NBT and riboflavin under illumination for 5 min in the absence and presence of different concentrations of (F) CeO_2, (G) Mn_3O_4, (H) PB, (I) PCN222-Mn, and (J) Pt NPs. (K) Dependence between the elimination efficiency of $^{\bullet}O_2^-$ and the concentrations of nanozymes, data analyzed from panels A–E. (L) Dependence between the elimination efficiency of $^{\bullet}O_2^-$ and the concentrations of nanozymes, data analyzed from panels F–J. A_0, the absorbance at 0 s; A, the absorbance at the corresponding time. The data are shown as means ± SD (n = 3).

reduced product and the detection sensitivity is necessary for the NBT probe.

On the other hand, by replacing the mixture of X and XO with the irradiation of riboflavin in the NBT based detection system, the SOD-like activities of these nanozymes as well as natural SODs were further investigated. As shown in Fig. 4F–J and L, all nanozymes showed SOD-like activities, meaning that this method has excellent detection sensitivity. Meanwhile, natural SODs showed a good positive correlation between concentrations and $^{\bullet}O_2^-$ eliminating activities (Fig. S6B and S6C†). However, compared with the results of the former enzyme based NBT probe (X, XO, and NBT), CeO_2 showed excellent SOD-like activity in this irradiation based NBT probe. This inconsistent result probably originates from the light-induced electron transfer between the excited riboflavin and CeO_2. Specifically, as a photosensitizer, riboflavin could transfer an electron to O_2 under irradiation, and thus produce $^{\bullet}O_2^-$. Meanwhile, CeO_2 is also known as an electron sponge which could accept an electron from the excited photosensitizer.[27] Therefore, CeO_2 could decrease the amount of $^{\bullet}O_2^-$ by seizing an electron from the excited photosensitizer. In this regard, taking into consideration the nanozymes' electron receiving capability in this detection system is necessary. As the detection system using the irradiation of riboflavin is more complex than the corresponding enzyme method, a mixture of X and XO was used in the subsequent experiments to produce $^{\bullet}O_2^-$.

INT, WST-8 and cytochrome *c*

As shown in Fig. 2, INT and WST-8 are the analogues of NBT, indicating that they could be reduced by $^{\bullet}O_2^-$ and produce colorimetric products. The differences among them are the water solubility and color of their reduced products. The reduced products of INT and WST-8 have better water solubility than that of NBT. Notably, WST-8 is also known as a commercial SOD assay kit. As shown in Fig. 5A–L, by comparing these analogues of NBT, the WST-8 probe showed excellent positive correlations between concentrations and SOD-like activities for these nanozymes, except for PB, meaning that the WST-8 probe has better detection sensitivity than others. Further detection for natural SODs demonstrated that the WST-8 probe indeed had a higher detection sensitivity than both the INT and NBT probes (Fig. S5C, S5D, and S5F†). However, the PB nanozyme didn't show SOD-like activity in these two probes, indicating the mismatched detection methods for PB nanozymes. Besides, the cytochrome *c* probe was further applied for evaluating the SOD-like activity of these nanozymes in the presence of X, XO and catalase (CAT). The detection method of cytochrome *c* involves the measurement of the absorbance changes at 550 nm, representing the newly generated Fe^{2+} which is formed from the reductive reaction between Fe^{3+} and $^{\bullet}O_2^-$. Because the as-formed Fe^{2+} is easily oxidized back to Fe^{3+} by H_2O_2, which is generated from $^{\bullet}O_2^-$, CAT is needed to

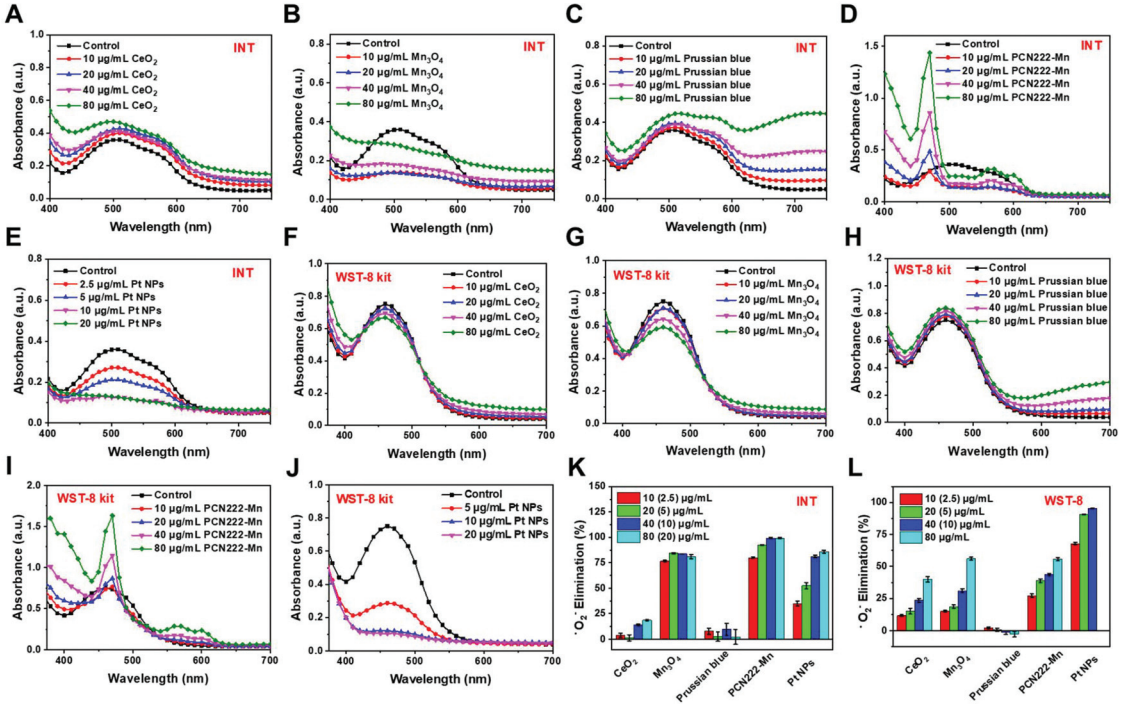

Fig. 5 Absorption spectra of the mixture of INT with X and XO in the absence and presence of different concentrations of (A) CeO_2, (B) Mn_3O_4, (C) PB, (D) PCN222-Mn, and (E) Pt NPs. Absorption spectra of the mixture of X, XO, and WST-8 in the absence and presence of different concentrations of (F) CeO_2, (G) Mn_3O_4, (H) PB, (I) PCN222-Mn, and (J) Pt NPs. (K) Dependence between the elimination efficiency of $^{\cdot}O_2^-$ and the concentrations of nanozymes, data analyzed from panels A–E. (L) Dependence between the elimination efficiency of $^{\cdot}O_2^-$ and the concentrations of nanozymes, data analyzed from panels F–J. A_0, the absorbance at 0 s; A, the absorbance at the corresponding time. The data are shown as means ± SD (n = 3).

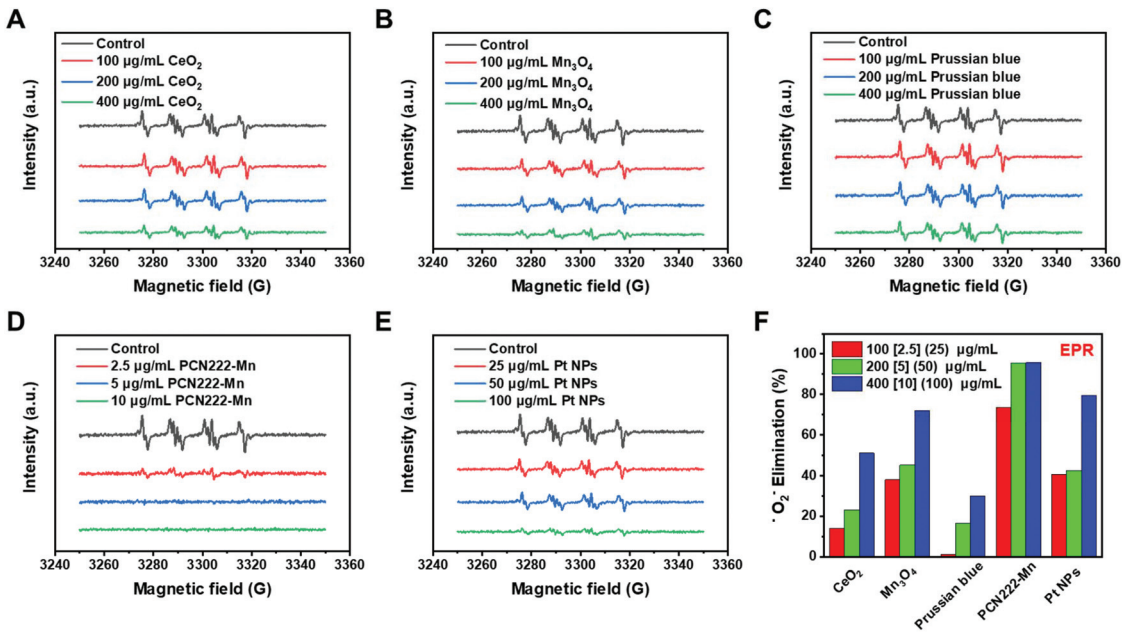

Fig. 6 EPR spectra of the mixed solution of X, XO, DMPO, and DTPA in the absence and presence of (A) CeO_2, (B) Mn_3O_4, (C) PB, (D) PCN222-Mn, and (E) Pt NPs with different concentrations. (F) Dependence between the elimination efficiency of $^{\cdot}O_2^-$ and the concentrations of nanozymes, data analyzed from panels A–E.

ensure the decomposition of H_2O_2. However, in our detection experiments, none of the nanozymes as well as natural SODs showed SOD-like activities in the cytochrome *c* based measurements (Fig. S4A–S4F and S5E†). These false negative results remind us that it is necessary to use more than one detection method for analyzing the SOD-like activities of nanozymes.

DMPO

Unlike the abovementioned probes, DMPO is a spin trapping reagent, which could form a covalent adduct with $^{\bullet}O_2^-$, and DMPO-$^{\bullet}O_2^-$, which rapidly converts to an adduct of DMPO-OOH in aqueous solution, thus making $^{\bullet}O_2^-$ detectable in the EPR spectrum. Due to the extremely short half-life of $^{\bullet}O_2^-$ in aqueous solution, the quality of DMPO as well as the incubation time are important factors for measuring $^{\bullet}O_2^-$ by EPR spectroscopy. As shown in Fig. S7,† the intensities of the hyperfine signals of DMPO-OOH decreased along with the increase of the incubation time from 10 s to 120 s, indicating that a short incubation time is beneficial for capturing the EPR signals. By using a 10 s incubation time, the SOD-like activities of nanozymes with different concentrations were then investigated (Fig. 6A). As shown in Fig. 6B, all nanozymes exhibited concentration-dependent $^{\bullet}O_2^-$ scavenging abilities, of which PCN222-Mn exhibited the highest SOD-like activity. Compared with other probes, EPR measurement is a more sensitive and accurate method for $^{\bullet}O_2^-$ detection, because it doesn't rely on the redox reactions with $^{\bullet}O_2^-$, thus avoiding the potential interference from the redox reactions between nanozymes and probes.

Conclusions

In this work, we have selected two $^{\bullet}O_2^-$ producing methods and six probes for evaluating the *in vitro* SOD-like activities of nanozymes. Five typical SOD-like nanozymes have been studied to compare the differences among these detection methods. According to the results, we found that the HE probe could be oxidized by nanozymes with oxidative abilities. Furthermore, the NBT probe has limited detection sensitivity owing to the poor water solubility of its reduced product. The WST-8 probe is an analogue of NBT but shows better detection sensitivity for nanozymes due to the good water solubility of its reduced product. Moreover, while using the irradiation of riboflavin to produce $^{\bullet}O_2^-$, the electron receiving capability of nanozymes needs to be considered. Lastly, EPR measurement is a more accurate method for the detection of SOD-like activity than others, whereas the quality of DMPO and the incubation time are important factors for producing EPR signals in aqueous solution. Based on the properties of nanozymes, using more than one method to detect their SOD-like activity would avoid the false positive or negative result. We hope this work would be useful to select a suitable and accurate *in vitro* detection method for evaluating the SOD-like activity of nanozymes in the future.

Conflicts of interest

There are no conflicts to declare.

Acknowledgements

This work was supported by the National Key R&D Program of China (2019YFA0709200), the National Natural Science Foundation of China (21722503 and 21874067), the PAPD Program, and the Fundamental Research Funds for the Central Universities (021314380145 and 021414380485). We thank Jia Yao for her initial efforts on this project and Christopher J. Butch for language editing.

Notes and references

1 K. Sugamura and J. F. Keaney Jr., *Free Radical Biol. Med.*, 2011, **51**, 978–992.
2 A. R. Bourgonje, M. Feelisch, K. N. Faber, A. Pasch, G. Dijkstra and H. van Goor, *Trends Mol. Med.*, 2020, **26**, 1034–1046.
3 J. Kim, H. Y. Kim, S. Y. Song, S.-h. Go, H. S. Sohn, S. Baik, M. Soh, K. Kim, D. Kim and H.-C. Kim, *ACS Nano*, 2019, **13**, 3206–3217.
4 H. Pelicano, D. Carney and P. Huang, *Drug Resist. Updates*, 2004, **7**, 97–110.
5 J. M. Matés, C. Pérez-Gómez and I. N. De Castro, *Clin. Biochem.*, 1999, **32**, 595–603.
6 R. A. Greenwald, *Free Radical Biol. Med.*, 1990, **8**, 201–209.
7 G. Seshadri, J. C. Sy, M. Brown, S. Dikalov, S. C. Yang, N. Murthy and M. E. Davis, *Biomaterials*, 2010, **31**, 1372–1379.
8 K. Salem, M. L. McCormick, E. Wendlandt, F. Zhan and A. Goel, *Redox Biol.*, 2015, **4**, 23–33.
9 K. Yasui and A. Baba, *Inflammation Res.*, 2006, **55**, 359–363.
10 D. P. Riley, *Chem. Rev.*, 1999, **99**, 2573–2588.
11 D. Salvemini, D. P. Riley and S. Cuzzocrea, *Nat. Rev. Drug Discovery*, 2002, **1**, 367–374.
12 L. Gao, J. Zhuang, L. Nie, J. Zhang, Y. Zhang, N. Gu, T. Wang, J. Feng, D. Yang, S. Perrett and X. Yan, *Nat. Nanotechnol.*, 2007, **2**, 577–583.
13 J. Wu, X. Wang, Q. Wang, Z. Lou, S. Li, Y. Zhu, L. Qin and H. Wei, *Chem. Soc. Rev.*, 2019, **48**, 1004–1076.
14 Y. Huang, J. Ren and X. Qu, *Chem. Rev.*, 2019, **119**, 4357–4412.
15 D. Jiang, D. Ni, Z. T. Rosenkrans, P. Huang, X. Yan and W. Cai, *Chem. Soc. Rev.*, 2019, **48**, 3683–3704.
16 Y. Zhang, M. Dai and Z. Yuan, *Anal. Methods*, 2018, **10**, 4625–4638.
17 M. Hayyan, M. A. Hashim and I. M. AlNashef, *Chem. Rev.*, 2016, **116**, 3029–3085.
18 H. J. Kwon, D. Kim, K. Seo, Y. G. Kim, S. I. Han, T. Kang, M. Soh and T. Hyeon, *Angew. Chem., Int. Ed.*, 2018, **57**, 9408–9412.
19 N. Singh, M. A. Savanur, S. Srivastava, P. D'Silva and G. Mugesh, *Angew. Chem., Int. Ed.*, 2017, **56**, 14267–14271.

20 W. Zhang, S. Hu, J. Yin, W. He, W. Lu, M. Ma, N. Gu and Y. Zhang, *J. Am. Chem. Soc.*, 2016, **138**, 5860–5865.
21 Y. Liu, Y. Cheng, H. Zhang, M. Zhou, Y. Yu, S. Lin, B. Jiang, X. Zhao, L. Miao, C. Wei, Q. Liu, Y. Lin, Y. Du, C. Butch and H. Wei, *Sci. Adv.*, 2020, **6**, eabb2695.
22 M. Kajita, K. Hikosaka, M. Iitsuka, A. Kanayama, N. Toshima and Y. Miyamoto, *Free Radical Res.*, 2007, **41**, 615–626.
23 H. T. Zhao, J. Joseph, H. M. Fales, E. A. Sokoloski, R. L. Levine, J. Vasquez-Vivar and B. Kalyanaraman, *Proc. Natl. Acad. Sci. U. S. A.*, 2005, **102**, 9086–9086.
24 H. S. Choi, J. W. Kim, Y. N. Cha and C. Kim, *J. Immunoassay Immunochem.*, 2006, **27**, 31–44.
25 S. Lin, Y. Cheng, H. Zhang, X. Wang, Y. Zhang, Y. Zhang, L. Miao, X. Zhao and H. Wei, *Small*, 2020, **16**, 1902123.
26 H. Ukeda, D. Kawana, S. Maeda and M. Sawamura, *Biosci. Biotechnol. Biochem.*, 1999, **63**, 485–488.
27 Y. Li, X. He, J.-J. Yin, Y. Ma, P. Zhang, J. Li, Y. Ding, J. Zhang, Y. Zhao, Z. Chai and Z. Zhang, *Angew. Chem., Int. Ed.*, 2015, **54**, 1832–1835.
28 R. A. Burgett, X. Bao and F. A. Villamena, *J. Phys. Chem. A*, 2008, **112**, 2447–2455.
29 J. Yao, Y. Cheng, M. Zhou, S. Zhao, S. Lin, X. Wang, J. Wu, S. Li and H. Wei, *Chem. Sci.*, 2018, **9**, 2927–2933.
30 J. Chen, Q. Wang, L. Huang, H. Zhang, K. Rong, H. Zhang and S. Dong, *Nano Res.*, 2018, **11**, 4905–4913.
31 M. A. Komkova, E. E. Karyakina and A. A. Karyakin, *J. Am. Chem. Soc.*, 2018, **140**, 11302–11307.
32 X. Wang, L. Qin, M. Zhou, Z. Lou and H. Wei, *Anal. Chem.*, 2018, **90**, 11696–11702.